

Spatial separation of the conformers of methyl vinyl ketone

Jia Wang,^{1, a)} Ardita Kilaj,² Lanhai He,^{1, b)} Karol Długołęcki,¹ Stefan Willitsch,^{2, c)} and Jochen Küpper^{1, 3, 4, d)}

¹⁾ Center for Free-Electron Laser Science, Deutsches Elektronen-Synchrotron DESY, Notkestrasse 85, 22607 Hamburg, Germany

²⁾ Department of Chemistry, University of Basel, Klingelbergstrasse 80, 4056 Basel, Switzerland

³⁾ Department of Physics, Universität Hamburg, Luruper Chaussee 149, 22761 Hamburg, Germany

⁴⁾ Center for Ultrafast Imaging, Universität Hamburg, Luruper Chaussee 149, 22761 Hamburg, Germany

(Dated: July 1, 2020)

Methyl vinyl ketone (C_4H_6O) is a volatile, labile organic compound of importance in atmospheric chemistry. We prepared a molecular beam of methyl vinyl ketone with a rotational temperature of 1.2(2) K and demonstrated the spatial separation of the *s-cis* and *s-trans* conformers of methyl vinyl ketone using the electrostatic deflector. The resulting sample density was $1.1 \times 10^8 \text{ cm}^{-3}$ for the direct beam in the laser ionization region. These conformer-selected methyl vinyl ketone samples are well suited for conformer specific chemical reactivity studies such as in Diels-Alder cycloaddition reactions.

I. INTRODUCTION

Methyl vinyl ketone (MVK, 3-butene-2-one, C_4H_6O) is the simplest α, β -unsaturated ketone and an important oxygenated volatile organic compound. MVK results from many sources such as vehicle exhaust,^{1,2} biomass burning³ and the ozonolysis of isoprene.⁴ As a primary first-yield product of isoprene oxidation in earth's atmosphere,^{5,6} MVK remains in the gas phase and is highly reactive.⁷ As a result, MVK has an important impact on the photochemical activity in the boundary layer, in particular in forested areas,⁸ and contributes to the destruction of ozone due to its formation of species such as formaldehyde and methylglyoxal.^{4,9} The atmospheric lifetime of MVK is $\sim 10 \text{ h}$ ^{8,10} due to its fast reaction with hydroxyl radicals under atmospheric conditions.¹¹ On the other hand, in the troposphere isoprene reacts with hydroxyl radicals and ozone molecules leading to a significant yield of MVK,¹² which is important for the formation of secondary organic aerosols and the overall NO_x cycle.^{9,13} Moreover, MVK is a candidate for prototypical pericyclic reactions, such as the Diels-Alder (DA) cycloaddition.^{14,15}

The ultraviolet absorption,¹⁶ microwave¹⁷⁻¹⁹ and infrared²⁰⁻²³ spectra of MVK provided evidence for a mixture of *s-cis* and *s-trans* MVK conformers and showed that *s-trans* MVK is more stable than *s-cis* MVK. Recently, the high-resolution rotational (7.5–18.5 GHz),²⁴ millimeter-wave,²⁵ and infrared spectra (540–6500 cm^{-1})²⁶ of MVK were reported. By combining experimental data and high-level quantum-chemistry calculations, the relative energy of *s-trans* MVK and *s-cis* MVK was determined as $164 \pm 30 \text{ cm}^{-1}$,²⁵ yielding an

equilibrium mixture of approximately 69 % *s-trans* MVK and 31 % *s-cis* MVK at room temperature.^{25,26}

The reactivity of different conformers, in spatially separated molecular beams, may vary significantly.^{27,28} Neutral molecules can be manipulated in the gas-phase using the electrostatic deflection technique,²⁹ which was demonstrated for the separation of individual quantum states,³⁰⁻³² conformers,³³⁻³⁷ or molecular clusters.³⁷⁻³⁹ This separation can be exploited for the investigation of the specific chemical reactivities of individual molecular species.^{27,40-42}

Here, we demonstrate the preparation of a cold and dense molecular beam of MVK and the spatial separation of the *s-cis* and *s-trans* conformers using the electrostatic deflector. Furthermore, we determine the density of the produced cold samples. The spatially separated conformers of MVK could be used for non-species-specific experiments, e.g., conformer-specific reactivity studies^{27,40} or ultrafast structural imaging experiments.⁴³⁻⁴⁵

II. EXPERIMENTAL SETUP

The experimental setup was described previously.^{36,46} A homebuilt gas handling system with a rotating high-pressure cylinder was added to fully and permanently mix MVK (Sigma-Aldrich, 99 %, used without further purification) and helium, see Fig. S1 in the supplementary information. The reservoir was filled with 2 ml of MVK, de-aired down to $\sim 10^{-2}$ mbar, and mixed with helium gas at 20 bar. The gas mixture was supersonically expanded through a cantilever piezo valve⁴⁷ operated at a repetition rate of 20 Hz. Two skimmers, placed 55 mm ($\varnothing = 3 \text{ mm}$) and 365 mm ($\varnothing = 1.5 \text{ mm}$) downstream of the valve were used to collimate the molecular beam, which was then directed through the electrostatic deflector²⁹ before passing through a third skimmer ($\varnothing = 1.5 \text{ mm}$) 562 mm downstream of the nozzle. MVK was ionized by a femtosecond laser with a wavelength centered at $\sim 800 \text{ nm}$ and a pulse duration of 45 fs (full-width at half maximum, FWHM) that was focused to 44 μm (FWHM) in the interaction region by a $f = 500 \text{ mm}$

^{a)}Permanent address: Department of Physics, Tsinghua University, 100084, Beijing, China

^{b)}Permanent address: Institute of Atomic and Molecular Physics, Jilin University, Changchun 130012, China

^{c)}Email: stefan.willitsch@unibas.ch

^{d)}Corresponding author. Email: jochen.kuepper@cfel.de; website: <https://www.controlled-molecule-imaging.org>

lens. The resulting ions were detected by a two-plate time-of-flight (TOF) mass spectrometer (MS).⁴⁸

III. RESULTS AND DISCUSSION

MVK is a liquid at room temperature and condenses on the sample reservoir walls, resulting in fast demixing of the prepared gas mixtures and corresponding fast decays of the MVK density in the molecular beam. Demixing was avoided through rotation of the sample reservoir (*vide supra*) and Figure 1 shows the resulting stability of the MVK signal following 20 h of sample rotation. Under these conditions the sample density was stable over a few hours and it decreased to 70 % over four days.

The normalized experimental vertical molecular beam profiles of MVK for different backing pressures of 2, 4, 6, and 8 bar are shown in Fig. S5 in the supplementary information. The full width of the direct molecular beam (0 kV) is 2 mm, determined by the skimmers and the distance between the third skimmer and ionization point. The deflected beam (10 kV) is deflected upward by ~ 0.8 mm when a pressure of 2 bar is applied to the piezo valve. Increasing the pressure to 4 bar, 6 bar, and 8 bar the deflection of the beam increases to ~ 1.0 mm, ~ 1.1 mm, and ~ 1.1 mm, respectively, which is due to the correspondingly lower rotational temperature of these beams.^{29,49}

Figure 2 a shows the experimental and simulated molecular beam profiles of MVK seeded in 8 bar of helium for deflector voltages of 0 V and 10 kV. The mass spectrum of the direct (0 kV) and deflected (10 kV) molecular beam are shown in Fig. S4 in the supplementary information. The spectrum of the deflected beam mainly contains signals from the MVK parent ion M^+ ($m/z = 70$) and from fragment ions $[M-CH_2=CH]^+$ ($m/z = 43$) and

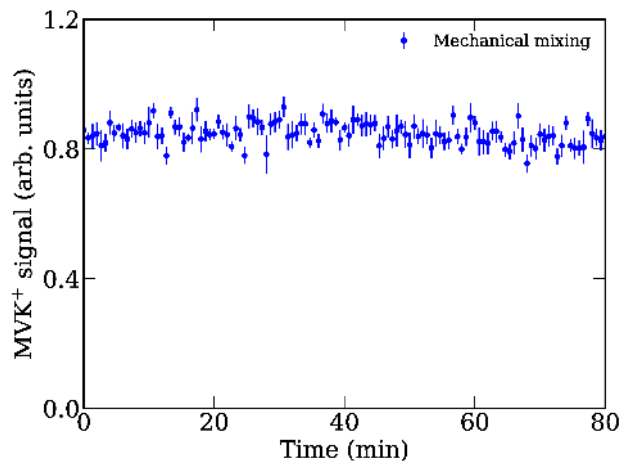


Figure 1. MVK signal over time for the sample preparation (200 ppm) of mechanical mixing by rotation of the sample cylinder.

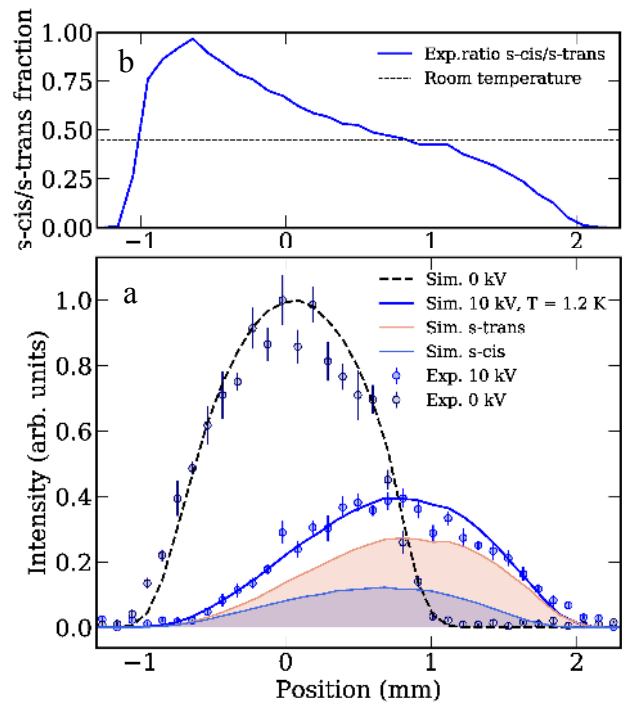


Figure 2. (a) Direct and deflected spatial beam profiles of MVK and simulation results. (b) The fractional population of the *s-cis* and *s-trans* conformer in the beam; the thin gray line depicts the ratio at room temperature [25, 26].

$[M-CH_3]^+$ ($m/z = 55$).

Solid and dotted lines in Figure 2 a show simulated spatial profiles using the molecular parameters and calculations detailed in the supplementary information. The effective dipole moments of the rotational states of *s-trans* are larger than ones of *s-cis* and, therefore, *s-trans* deflects further than *s-cis*. Assuming a thermal distribution of the population of rotational states, the best fit for the profile of MVK in Figure 2 was obtained for a rotational temperature of 1.2(2) K. The deflection and simulation profiles of MVK seeded in different pressures of helium are shown in Fig. S3 in the supplementary information.

Although no full separation was possible, *s-trans* MVK was deflected more than *s-cis* MVK. The fractional contributions of the conformers across the vertical beam profile are shown in Figure 2 b, assuming the same excitation and ionization cross-sections for the two conformers.³⁵ A beam of *s-trans* conformer with a purity higher than 90 % was obtained for vertical molecular-beam positions $y \geq 1.9$ mm.

The MVK sample densities in the experiments were estimated based on a strong-field ionization model.^{50,51} Assuming an instrument sensitivity of 50 % for the MCP detector⁵² the asymptotic slope of an integral ionization signal with respect to the natural logarithm of peak intensity can be expressed as $S = \varrho\pi\sigma^2D$,^{50,51} where

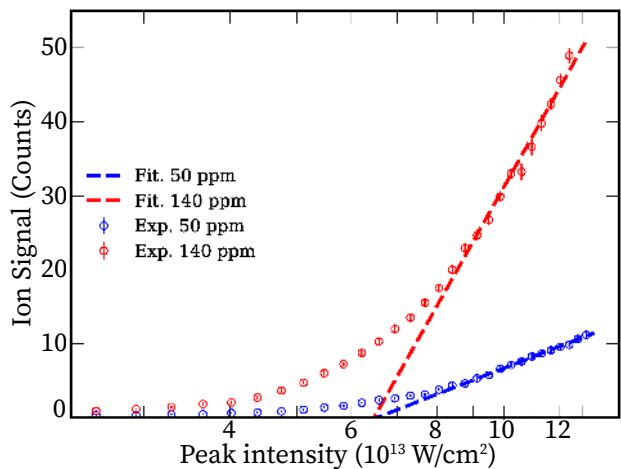


Figure 3. The MVK signal count (per shot) versus the peak intensity on a semi-logarithmic scale (dots). MVK samples are seeded in 2 bar of He with ratios of 50 ppm (blue) and 140 ppm (red). The dashed lines are the linear fitting of the asymptotic behaviour.

ρ represents the sample density, σ the standard deviation of the transverse intensity distribution and D the length of the focal volume in the molecular beam. The MVK signal count *versus* the peak intensity are shown on a semi-logarithmic scale in Figure 3, where the sum of the signals of the parent ion ($m/z = 70$) and its fragments ($m/z = 43$ and $m/z = 55$) was used. The saturation onset was deduced for a laser peak intensity $I_{\text{sat}} = 6.5 \times 10^{13} \text{ W/cm}^2$ for mixing ratios of MVK sample and helium of 50 and 140 ppm. For the known laser focus $\sigma = 22 \text{ }\mu\text{m}$ and a molecular-beam diameter of $D = 2 \text{ mm}$, the sample densities in the laser ionization region, $\sim 750 \text{ mm}$ downstream the valve, were $2.4 \times 10^7 \text{ cm}^{-3}$ and $1.1 \times 10^8 \text{ cm}^{-3}$, respectively.

IV. CONCLUSION

We demonstrated the use of a rotating-sample reservoir for the production of a dense and cold molecular beam of MVK with stable molecular densities over more than a day and a rotational temperature of 1.2(2) K. This allowed for the spatial dispersion and partial separation of the *s-cis* and *s-trans* conformers of MVK using the electrostatic deflector. The achieved direct-beam density in the detection zone was experimentally determined to be $1.1 \times 10^8 \text{ cm}^{-3}$.

We plan to exploit these conformer-selected MVK samples for reactivity studies, e.g., with the ions of MVK (self-reaction), methyl vinyl ether, and further dienophile cations, to investigate the mechanism and conformational specificities of ionic Diels-Alder (DA) cycloaddition reactions.⁵³ Furthermore, the reactivity of the conformers in reactions with neutral atmospheric molecules, such

as OH, would be extremely interesting for atmospheric chemistry applications.

SUPPLEMENTARY MATERIAL

See the supplementary material for a schematic of the gas panel, the direct and deflected molecular beam profiles of MVK for different backing pressures, the mass spectra obtained in the direct and the deflected molecular beams, the rotational constants and dipole moments of the MVK conformers, their Stark energies, and the deflection and simulation profiles of MVK seeded in helium of different pressures.

ACKNOWLEDGMENTS

We acknowledge help with the experimental setup by Jovana Petrović and Nicolai Pohlmann. This work has been supported by the cluster of excellence “Advanced Imaging of Matter” (AIM, EXC 2056, ID 390715994) of the Deutsche Forschungsgemeinschaft (DFG), by the European Research Council under the European Union’s Seventh Framework Program (FP7/2007-2013) through the Consolidator Grant COMOTION (614507), and by the Swiss National Science Foundation under grants nr. BSCGI0_157874 and IZCOZO_189907. J.W. and L.H. acknowledge fellowships within the framework of the Helmholtz-OCPC postdoctoral exchange program.

REFERENCES

- ¹T. A. Biesenthal and P. B. Shepson, “Observations of anthropogenic inputs of the isoprene oxidation products methyl vinyl ketone and methacrolein to the atmosphere,” *Geophys. Res. Lett.* **24**, 1375–1378 (1997).
- ²D. Zhang, W. Lei, and R. Zhang, “Mechanism of OH formation from ozonolysis of isoprene: kinetics and product yields,” *Chem. Phys. Lett.* **358**, 171 – 179 (2002).
- ³F. Brilli, B. Gioli, P. Ciccioli, D. Zona, F. Loreto, I. A. Janssens, and R. Ceulemans, “Proton transfer reaction time-of-flight mass spectrometric (PTR-TOF-MS) determination of volatile organic compounds (VOCs) emitted from a biomass fire developed under stable nocturnal conditions,” *Atmos. Environ.* **97**, 54 – 67 (2014).
- ⁴R. Gutbrod, E. Kraka, R. N. Schindler, and D. Cremer, “Kinetic and theoretical investigation of the gas-phase ozonolysis of isoprene: Carbonyl oxides as an important source for OH radicals in the atmosphere,” *J. Am. Chem. Soc.* **119**, 7330–7342 (1997).
- ⁵E. C. Tuazon and R. Atkinson, “A product study of the gas-phase reaction of methyl vinyl ketone with the OH radical in the presence of NO_x ,” *Int. J. Chem. Kinet.* **21**, 1141–1152 (1989).
- ⁶M. M. Galloway, A. J. Huisman, L. D. Yee, A. W. H. Chan, C. L. Loza, J. H. Seinfeld, and F. N. Keutsch, “Yields of oxidized volatile organic compounds during the OH radical initiated oxidation of isoprene, methyl vinyl ketone, and methacrolein under high- NO_x conditions,” *Atmos. Chem. Phys.* **11**, 10779–10790 (2011).
- ⁷D. Pierotti, S. C. Wofsy, D. Jacob, and R. A. Rasmussen, “Isoprene and its oxidation products: Methacrolein and methyl vinyl ketone,” *J. Geophys. Res. Atmos.* **95**, 1871–1881 (1990).

- ⁸M. Karl, H.-P. Dorn, F. Holland, R. Koppmann, D. Poppe, L. Rupp, A. Schaub, and A. Wahner, "Product study of the reaction of OH radicals with isoprene in the atmosphere simulation chamber SAPHIR," *J. Atmos. Chem.* **55**, 167–187 (2006).
- ⁹E. Praske, J. D. Crounse, K. H. Bates, T. Kurtén, H. G. Kjaergaard, and P. O. Wennberg, "Atmospheric fate of methyl vinyl ketone: Peroxy radical reactions with NO and HO₂," *J. Phys. Chem. A* **119**, 4562–4572 (2015), PMID: 25486386.
- ¹⁰R. Atkinson, D. L. Baulch, R. A. Cox, J. N. Crowley, R. F. Hampson, R. G. Hynes, M. E. Jenkin, M. J. Rossi, J. Troe, and I. Subcommittee, "Evaluated kinetic and photochemical data for atmospheric chemistry: Volume II - gas phase reactions of organic species," *Atmos. Chem. Phys.* **6**, 3625–4055 (2006).
- ¹¹R. Atkinson, "Kinetics and mechanisms of the gas-phase reactions of the hydroxyl radical with organic compounds under atmospheric conditions," *Chem. Rev.* **86**, 69–201 (1986).
- ¹²S. M. Aschmann and R. Atkinson, "Formation yields of methyl vinyl ketone and methacrolein from the gas-phase reaction of O₃ with isoprene," *Environ. Sci. Technol.* **28**, 1539–1542 (1994).
- ¹³J. H. Kroll and J. H. Seinfeld, "Chemistry of secondary organic aerosol: Formation and evolution of low-volatility organics in the atmosphere," *Atmos. Environ.* **42**, 3593–3624 (2008).
- ¹⁴W. L. Jorgensen, D. Lim, and J. F. Blake, "Ab initio study of diels-alder reactions of cyclopentadiene with ethylene, isoprene, cyclopentadiene, acrylonitrile, and methyl vinyl ketone," *J. Am. Chem. Soc.* **115**, 2936–2942 (1993).
- ¹⁵W. L. Jorgensen, J. F. Blake, D. Lim, and D. L. Severance, "Investigation of solvent effects on pericyclic reactions by computer simulations," *J. Chem. Soc., Faraday Trans.* **90**, 1727–1732 (1994).
- ¹⁶M. T. Rogers, "The electric moments and ultraviolet absorption spectra of some derivatives of cyclopropane and of ethylene oxide," *J. Am. Chem. Soc.* **69**, 2544–2548 (1947).
- ¹⁷P. D. Foster, V. M. Rao, and R. F. Curl Jr, "Microwave spectrum of methyl vinyl ketone," *J. Chem. Phys.* **43**, 1064–1066 (1965).
- ¹⁸A. Fantoni, W. Caminati, and R. Meyer, "Torsional interactions in methyl vinyl ketone," *Chem. Phys. Lett.* **133**, 27–33 (1987).
- ¹⁹J. De Smedt, F. Vanhouteghem, C. Van Alsenoy, H. Geise, B. Van der Veken, and P. Coppens, "Methyl vinyl ketone in the gas phase, investigated by electron diffraction, infrared band contour analysis and microwave spectroscopy, supplemented with ab initio calculations of geometries and force fields," *J. Mol. Struct.* **195**, 227–251 (1989).
- ²⁰K. Noack and R. N. Jones, "Conformational equilibria in open-chain α , β -unsaturated ketones," *Can. J. Chem.* **39**, 2225–2235 (1961).
- ²¹A. Bowles, W. George, and W. Maddams, "Conformations of some α , β -unsaturated carbonyl compounds. Part I. infrared spectra of acraldehyde, crotonaldehyde, methyl vinyl ketone, and ethylideneacetone," *J. Chem. Soc. B*, 810–818 (1969).
- ²²J. Durig and T. Little, "Conformational barriers to internal rotation and vibrational assignment of methyl vinyl ketone," *J. Chem. Phys.* **75**, 3660–3668 (1981).
- ²³H.-J. Oelichmann, D. Bougeard, and B. Schrader, "Coupled calculation of vibrational frequencies and intensities: Part VI. IR and raman spectra of crotonaldehyde, methacrolein and methylvinylketone," *J. Mol. Struct.* **77**, 179–194 (1981).
- ²⁴D. S. Wilcox, A. J. Shirar, O. L. Williams, and B. C. Dian, "Additional conformer observed in the microwave spectrum of methyl vinyl ketone," *Chem. Phys. Lett.* **508**, 10–16 (2011).
- ²⁵O. Zakharenko, R. A. Motiyenko, J. R. Aviles Moreno, and T. R. Huet, "Conformational landscape and torsion-rotation-vibration effects in the two conformers of methyl vinyl ketone, a major oxidation product of isoprene," *J. Phys. Chem. A* **121**, 6420–6428 (2017).
- ²⁶R. Lindenmaier, S. D. Williams, R. L. Sams, and T. J. Johnson, "Quantitative infrared absorption spectra and vibrational assignments of crotonaldehyde and methyl vinyl ketone using gas-phase mid-infrared, far-infrared, and liquid raman spectra: *s-cis* vs *s-trans* composition confirmed via temperature studies and ab initio methods," *J. Phys. Chem. A* **121**, 1195–1212 (2017).
- ²⁷Y.-P. Chang, K. Długołęcki, J. Küpper, D. Rösch, D. Wild, and S. Willitsch, "Specific chemical reactivities of spatially separated 3-aminophenol conformers with cold Ca⁺ ions," *Science* **342**, 98–101 (2013), arXiv:1308.6538 [physics].
- ²⁸S. Willitsch, "Chemistry with controlled ions," *Adv. Chem. Phys.* **162**, 307 (2017).
- ²⁹Y.-P. Chang, D. A. Horke, S. Trippel, and J. Küpper, "Spatially-controlled complex molecules and their applications," *Int. Rev. Phys. Chem.* **34**, 557–590 (2015), arXiv:1505.05632 [physics].
- ³⁰J. H. Nielsen, P. Simesen, C. Z. Bisgaard, H. Stapelfeldt, F. Filsinger, B. Friedrich, G. Meijer, and J. Küpper, "Stark-selected beam of ground-state OCS molecules characterized by revivals of impulsive alignment," *Phys. Chem. Chem. Phys.* **13**, 18971–18975 (2011), arXiv:1105.2413 [physics].
- ³¹D. A. Horke, Y.-P. Chang, K. Długołęcki, and J. Küpper, "Separating para and ortho water," *Angew. Chem. Int. Ed.* **53**, 11965–11968 (2014), arXiv:1407.2056 [physics].
- ³²J. S. Kienitz, K. Długołęcki, S. Trippel, and J. Küpper, "Improved spatial separation of neutral molecules," *J. Chem. Phys.* **147**, 024304 (2017), arXiv:1704.08912 [physics].
- ³³F. Filsinger, U. Erlekam, G. von Helden, J. Küpper, and G. Meijer, "Selector for structural isomers of neutral molecules," *Phys. Rev. Lett.* **100**, 133003 (2008), arXiv:0802.2795 [physics].
- ³⁴F. Filsinger, J. Küpper, G. Meijer, J. L. Hansen, J. Maurer, J. H. Nielsen, L. Holmegaard, and H. Stapelfeldt, "Pure samples of individual conformers: the separation of stereo-isomers of complex molecules using electric fields," *Angew. Chem. Int. Ed.* **48**, 6900–6902 (2009).
- ³⁵T. Kierspel, D. A. Horke, Y.-P. Chang, and J. Küpper, "Spatially separated polar samples of the *cis* and *trans* conformers of 3-fluorophenol," *Chem. Phys. Lett.* **591**, 130–132 (2014), arXiv:1312.4417 [physics].
- ³⁶N. Teschmit, D. A. Horke, and J. Küpper, "Spatially separating the conformers of a dipeptide," *Angew. Chem. Int. Ed.* **57**, 13775–13779 (2018), arXiv:1805.12396 [physics].
- ³⁷H. S. You, J. Kim, S. Han, D.-S. Ahn, J. S. Lim, and S. K. Kim, "Spatial isolation of conformational isomers of hydroquinone and its water cluster using the stark deflector," *J. Phys. Chem. A* **122**, 1194 (2018).
- ³⁸S. Trippel, Y.-P. Chang, S. Stern, T. Mullins, L. Holmegaard, and J. Küpper, "Spatial separation of state- and size-selected neutral clusters," *Phys. Rev. A* **86**, 033202 (2012), arXiv:1208.4935 [physics].
- ³⁹M. Johny, J. Onvlee, T. Kierspel, H. Bieker, S. Trippel, and J. Küpper, "Spatial separation of pyrrole and pyrrole-water clusters," *Chem. Phys. Lett.* **721**, 149–152 (2019), arXiv:1901.05267 [physics].
- ⁴⁰A. Kilaj, H. Gao, D. Rösch, U. Rivero, J. Küpper, and S. Willitsch, "Observation of different reactivities of para- and ortho-water towards trapped diazenylium ions," *Nat. Commun.* **9**, 2096 (2018).
- ⁴¹D. Rösch, S. Willitsch, Y.-P. Chang, and J. Küpper, "Chemical reactions of conformationally selected 3-aminophenol molecules in a beam with coulomb-crystallized ca⁺ ions," *J. Chem. Phys.* **140**, 124202 (2014).
- ⁴²A. Kilaj, H. Gao, D. Tahchieva, R. Ramakrishnan, D. Bachmann, D. Gillingham, O. A. von Lilienfeld, J. Küpper, and S. Willitsch, "Quantum-chemistry-aided identification, synthesis and experimental validation of model systems for conformationally controlled reaction studies: Separation of the conformers of 2,3-dibromobuta-1,3-diene in the gas phase," *Phys. Chem. Chem. Phys.* **22**, 13431–13439 (2020), arXiv:2004.09659 [physics].
- ⁴³J. Küpper, S. Stern, L. Holmegaard, F. Filsinger, A. Rouzée, A. Rudenko, P. Johnsson, A. V. Martin, M. Adolph, A. Aquila, S. Bajt, A. Barty, C. Bostedt, J. Bozek, C. Caleman, R. Coffee, N. Coppola, T. Delmas, S. Epp, B. Erk, L. Foucar, T. Gorkhover, L. Gumprecht, A. Hartmann, R. Hartmann, G. Hauser, P. Holl, A. Hömke, N. Kimmel, F. Krasniqi, K.-U. Kühnel, J. Maurer, M. Messerschmidt, R. Moshhammer, C. Re-

- ich, B. Rudek, R. Santra, I. Schlichting, C. Schmidt, S. Schorb, J. Schulz, H. Soltau, J. C. H. Spence, D. Starodub, L. Strüder, J. Thøgersen, M. J. J. Vrakking, G. Weidenspointner, T. A. White, C. Wunderer, G. Meijer, J. Ullrich, H. Stapelfeldt, D. Rolles, and H. N. Chapman, “X-ray diffraction from isolated and strongly aligned gas-phase molecules with a free-electron laser,” *Phys. Rev. Lett.* **112**, 083002 (2014), arXiv:1307.4577 [physics].
- ⁴⁴C. J. Hensley, J. Yang, and M. Centurion, “Imaging of isolated molecules with ultrafast electron pulses,” *Phys. Rev. Lett.* **109**, 133202 (2012).
- ⁴⁵J. Wiese, J. Onvlee, S. Trippel, and J. Küpper, “Strong-field ionization of complex molecules,” (2020), under review, arXiv:2003.02116 [physics].
- ⁴⁶J. Wang, L. He, J. Petrovic, A. Al-Refaie, H. Bieker, J. Onvlee, K. Długołęcki, and J. Küpper, “Spatial separation of 2-propanol monomer and its ionization-fragmentation pathways,” *J. Mol. Struct.* **1208**, 127863 (2020).
- ⁴⁷D. Irimia, D. Dobrikov, R. Kortekaas, H. Voet, D. A. van den Ende, W. A. Groen, and M. H. M. Janssen, “A short pulse (7 μ s FWHM) and high repetition rate (dc–5kHz) cantilever piezovalve for pulsed atomic and molecular beams,” *Rev. Sci. Instrum.* **80**, 113303 (2009).
- ⁴⁸J. S. Kienitz, S. Trippel, T. Mullins, K. Długołęcki, R. González-Férez, and J. Küpper, “Adiabatic mixed-field orientation of ground-state-selected carbonyl sulfide molecules,” *Chem. Phys. Chem.* **17**, 3740–3746 (2016), arXiv:1607.05615 [physics].
- ⁴⁹F. Filsinger, J. Küpper, G. Meijer, L. Holmegaard, J. H. Nielsen, I. Nevo, J. L. Hansen, and H. Stapelfeldt, “Quantum-state selection, alignment, and orientation of large molecules using static electric and laser fields,” *J. Chem. Phys.* **131**, 064309 (2009), arXiv:0903.5413 [physics].
- ⁵⁰S. Hankin, D. Villeneuve, P. Corkum, and D. Rayner, “Intense-field laser ionization rates in atoms and molecules,” *Phys. Rev. A* **64**, 013405 (2001).
- ⁵¹J. Wiese, J.-F. Olivieri, A. Trabattoni, S. Trippel, and J. Küpper, “Strong-field photoelectron momentum imaging of OCS at finely resolved incident intensities,” *New J. Phys.* **21**, 083011 (2019), arXiv:1904.07519 [physics].
- ⁵²K. Fehre, D. Trojanowskaja, J. Gatzke, M. Kunitski, F. Trinter, S. Zeller, L. P. H. Schmidt, J. Stohner, R. Berger, A. Czasch, O. Jagutzki, T. Jahnke, R. Dörner, and M. S. Schöffler, “Absolute ion detection efficiencies of microchannel plates and funnel microchannel plates for multi-coincidence detection,” *Rev. Sci. Instrum.* **89**, 045112 (2018).
- ⁵³U. Rivero, M. Meuwly, and S. Willitsch, “A computational study of the diels-alder reactions between 2,3-dibromo-1,3-butadiene and maleic anhydride,” *Chem. Phys. Lett.* **683**, 598 – 605 (2017), ahmed Zewail (1946-2016) Commemoration Issue of Chemical Physics Letters.

Supplemental Material: Spatial separation of the conformers of methyl vinyl ketone

Jia Wang,^{1, a)} Ardita Kilaj,² Lanhai He,^{1, b)} Karol Długołęcki,¹ Stefan Willitsch,^{2, c)} and Jochen Küpper^{1, 3, 4, d)}

¹⁾ Center for Free-Electron Laser Science, Deutsches Elektronen-Synchrotron DESY, Notkestrasse 85, 22607 Hamburg, Germany

²⁾ Department of Chemistry, University of Basel, Klingelbergstrasse 80, 4056 Basel, Switzerland

³⁾ Department of Physics, Universität Hamburg, Luruper Chaussee 149, 22761 Hamburg, Germany

⁴⁾ Center for Ultrafast Imaging, Universität Hamburg, Luruper Chaussee 149, 22761 Hamburg, Germany

(Dated: July 1, 2020)

I. SAMPLE PREPARATION

MVK is a liquid with a relatively high vapor pressure of ~ 130 mbar at room temperature and its vapor/air mixtures are explosive. Figure S1 shows the schematic of the gas panel for sample preparation. This includes the pumping system, pipes, the MVK reservoir, and a rotating sample cylinder. The sample cylinder is mounted on a rotating motor (DGM130R-AZAC, Oriental Motor) and is connected by soft PEEK tubes. The 2 ml MVK sample is filled into the MVK reservoir and de-aired. First, the whole gas line is evacuated (HiCube Eco, Pfeiffer Vacuum) to $\sim 10^{-2}$ mbar, then MVK vapor is leaked into the sample cylinder to the designed pressure, and subsequently filled with helium to 20 bar. The cylinder is closed and rotated. To minimize corrosion the MVK sample is removed from the gas lines and the sample reservoir

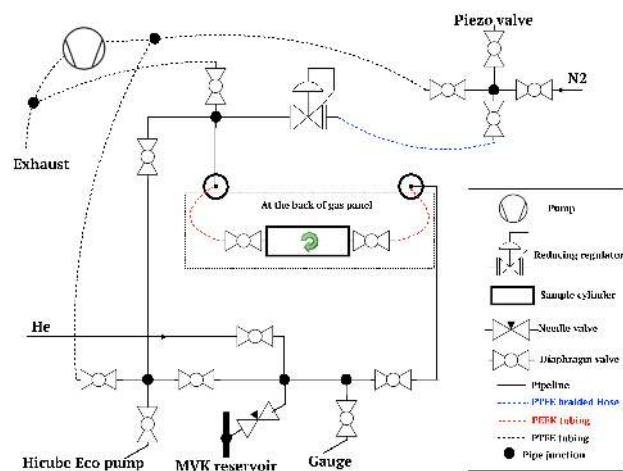


Figure S1. Schematic of the gas handling system, see text for details.

^{a)} Permanent address: Department of Physics, Tsinghua University, 100084, Beijing, China

^{b)} Permanent address: Institute of Atomic and Molecular Physics, Jilin University, Changchun 130012, China

^{c)} Email: stefan.willitsch@unibas.ch

^{d)} Email: jochen.kuepper@cfel.de; website: <https://www.controlled-molecule-imaging.org>

when not used.

II. STARK ENERGY CALCULATIONS AND NUMERICAL SIMULATIONS

The Stark energies for all rotational states of both conformers of MVK up to $J = 15$ were calculated in a basis of all field-free rotational states with $J \leq 30$ using the freely available CMISTARK software package.⁷ The rotational constants and dipole moments of *s-cis* MVK and *s-trans* MVK^{7, 8} are summarized in Table S1. The Stark curves of the lowest-energy rotational states are shown in Figure S2.

Figure S3 shows the normalized experimental and simulated vertical molecular beam profiles of MVK seeded in 2, 4, 6, and 8 bar of helium, for voltages to the deflector of 0 V and 10 kV. The mixing ratio MVK/helium of the sample was 200 ppm. Solid and dotted lines in Figure S3 show simulated spatial profiles of the individual conformers. We simulated $\times 10^5$ classical trajectories for every quantum state with $J \leq 14$ and the experimental parameters.^{7, 8} Assuming a Boltzmann population distribution of rotational states, the rotational temperatures of MVK seeded in helium of different pressures (2, 4, 6, 8 bar) were fitted to be 7.5, 3.5, 1.5, and 1.2 K.

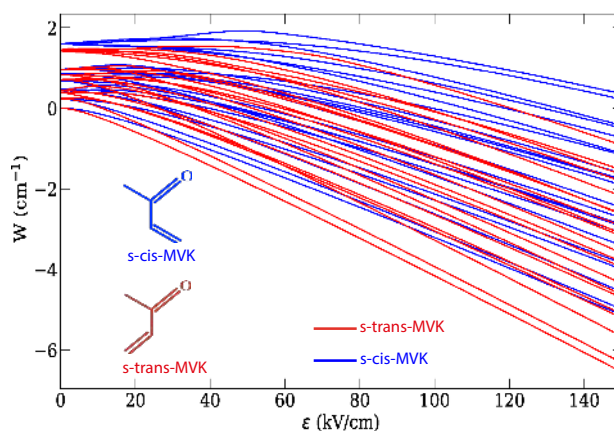


Figure S2. The calculated adiabatic Stark energies of the lowest-energy rotational states ($J = 0 \dots 2$) of MVK in a dc electric field.

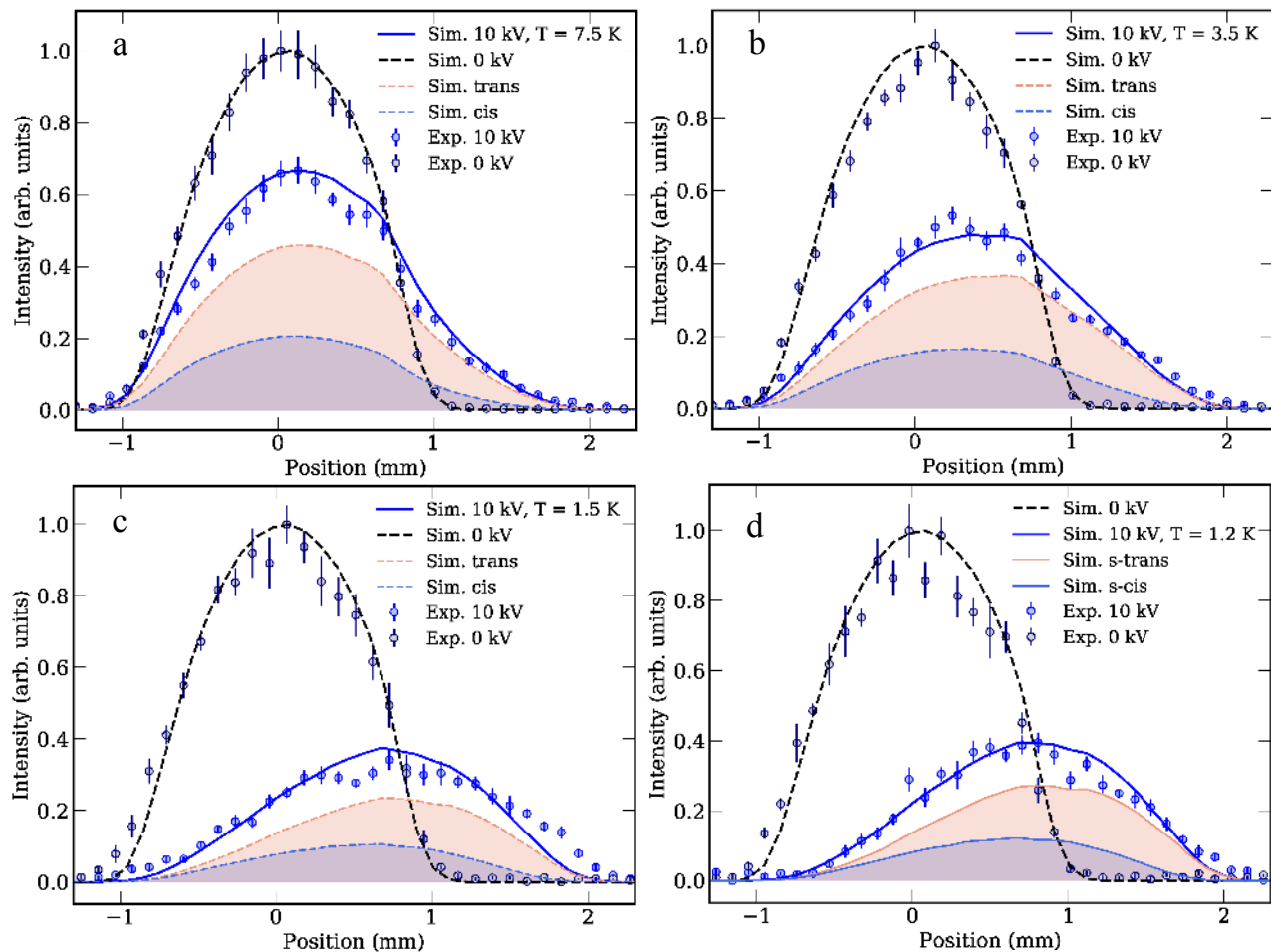


Figure S3. Experimental and simulated deflection profiles of MVK seeded in helium at different pressures of (a) 2 bar, (b) 4 bar, (c) 6 bar, and (d) 8 bar.

Table S1. Rotational constants and dipole moment components^{??} used for the Stark effect calculations.

	<i>s-cis</i> conformer	<i>s-trans</i> conformer
A (MHz)	10240.938	8941.590
B (MHz)	3991.6351	4274.5443
C (MHz)	2925.648	2945.3315
μ_A (D)	-0.57	2.53
μ_B (D)	2.88	-1.91
μ_C (D)	0	0

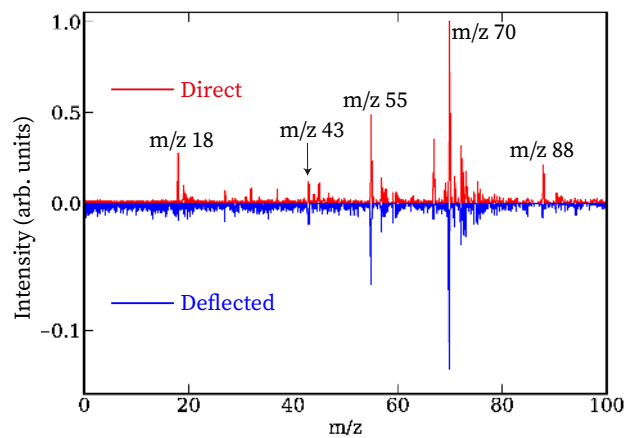


Figure S4. Mass spectrum of the direct (0 kV) and deflected (10 kV) molecular beam, corresponding to the positions at 0 mm and 1.65 mm in Figure 2 in the main manuscript. The spectra were normalized to the monomer ion signal ($m/z = 70$). No ion signal was found above $m/z = 100$.

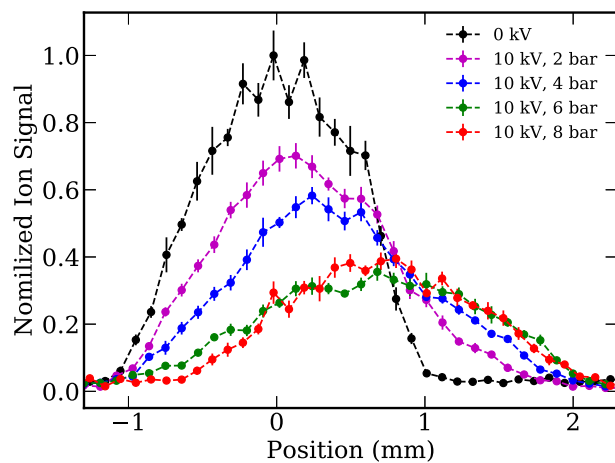


Figure S5. Vertical profiles of the direct (0 kV) and deflected (10 kV) molecular beam of MVK for different backing pressures applied to the piezo valve.